

# INTERNATIONAL SOCIETY FOR SOIL MECHANICS AND GEOTECHNICAL ENGINEERING



*This paper was downloaded from the Online Library of the International Society for Soil Mechanics and Geotechnical Engineering (ISSMGE). The library is available here:*

<https://www.issmge.org/publications/online-library>

*This is an open-access database that archives thousands of papers published under the Auspices of the ISSMGE and maintained by the Innovation and Development Committee of ISSMGE.*

*The paper was published in the proceedings of the 20<sup>th</sup> International Conference on Soil Mechanics and Geotechnical Engineering and was edited by Mizanur Rahman and Mark Jaksa. The conference was held from May 1<sup>st</sup> to May 5<sup>th</sup> 2022 in Sydney, Australia.*

## A pragmatic approach to estimating earthquake design spectra for structures on deep foundations

Une approche pragmatique pour estimer les spectres de conception de tremblements de terre pour les structures sur fondations profondes

**Antony Orton, Harry Poulos & Patrick Wong**

*Tetra Tech Coffey Pty Ltd*

**ABSTRACT:** Earthquake design spectra for structures are generally based on the geotechnical characteristics of a site and usually do not consider the nature of the foundation supporting the structure. In this paper, a pragmatic approach is outlined for considering the effect of a deep foundation on the design response spectrum. This approach involves the following key steps:

1. Characterisation of the site and the assignment of appropriate stiffness and damping characteristics to the strata;
2. Identification of relevant earthquakes on the basis of magnitude, peak bedrock acceleration and epicentral distance from the causative fault(s);
3. Carrying out of site response analyses for each earthquake ground motion record, and the calculation of the base and surface response spectra;
4. Averaging of these spectra to obtain representative surface and base spectra;
5. Correction of the representative surface spectrum via published correction factors related to the characteristics of the deep foundation.

The paper describes briefly the authors' program ERLS which is written in the Python programming language. This program is verified via comparisons with analytic solutions and the publicly available program DEEPSOIL. ERLS carries out the averaging of a series of spectra for various earthquake records and then applies a deep foundation correction factor to obtain the final response spectrum for the pile-supported structure.

**RÉSUMÉ:** Les spectres de conception de tremblement de terre pour les structures sont généralement basés sur les caractéristiques géotechniques d'un site et ne tiennent généralement pas compte de la nature de la fondation supportant la structure. Dans cet article, une approche pragmatique est décrite pour considérer l'effet d'une fondation profonde sur le spectre de réponse de conception. Cette approche comprend les étapes clés suivantes:

1. Caractérisation du site et attribution de caractéristiques de rigidité et d'amortissement appropriées aux strates;
2. Identification des tremblements de terre pertinents sur la base de la magnitude, de l'accélération maximale du substrat rocheux et de la distance épicentrale de la ou des failles causales;
3. La réalisation d'analyses de réponse du site pour chaque enregistrement de mouvement du sol sismique, et le calcul des spectres de réponse de base et de surface;
4. La moyenne de ces spectres pour obtenir des spectres de surface et de base représentatifs;
5. La correction du spectre de surface représentatif via des facteurs de correction publiés liés aux caractéristiques de la fondation profonde.

L'article décrit brièvement le programme des auteurs ERLS qui est écrit dans le langage de programmation Python. Ce programme est vérifié via des comparaisons avec des solutions analytiques et le programme public DEEPSOIL. ERLS effectue le moyennage d'une série de spectres pour divers enregistrements de tremblements de terre, puis applique un facteur de correction de fondations profondes pour obtenir le spectre de réponse final pour la structure sur pieux.

**KEYWORDS:** Earthquake; finite difference analysis; piles; response spectra; site response

### 1 INTRODUCTION

It is common in engineering practice to adopt site response spectra for buildings on deep foundations by ignoring the filtering effects provided by the foundations, with the free field motion response spectra usually being used instead. This ignores the beneficial effects that piles often provide, especially in reducing seismic loads in the high frequency range.

This paper sets out methods for incorporating the effects of piles on seismic site response spectra for use in routine design. These methods are based on the results of parametric studies undertaken by several authors and provide factors that are applied to the free field motion response spectra. The factors take into account the properties of the pile foundation, the frequency content of the input earthquake, and/or the frequency content of the resulting free-field motion.

A brief description of the approach used to derive the free-field motion and the application of the deep foundation factor is provided, including a discussion of the use of the Python programming language in the analysis.

An application of the methodology to a project in Sydney is described. This includes a discussion of the characterisation of the site, how the relevant parameters were obtained, and the selection of input earthquake records and their details. A comparison of the response spectra obtained using the various methods of incorporating deep foundations is then presented.

### 2 SITE RESPONSE ANALYSIS

Typically, earthquake ground motion records are available for monitoring points on rock outcrops. Conversely, engineering

projects are often constructed on sites consisting of soil overlying bedrock. The purpose of a site response analysis is to account for the effects of the soil in modifying the earthquake ground motion as it travels from the underlying bedrock to the ground surface.

The key parameter affecting the seismic amplification is the shear wave velocity ( $V_s$ ) of the soil. The shear wave velocity is directly related to the small strain shear modulus ( $G_0$ ) and the density ( $\rho$ ) using the equation:

$$G_0 = \rho V_s^2 \quad (1)$$

The other important soil parameter is the soil damping ratio, which is related to the energy dissipation in the soil.

Each site has a natural site period equal to:

$$T_n = \frac{4H}{V_{s,avg}} \quad (2)$$

with  $H$  usually taken as the depth to bedrock.  $V_{s,avg}$  is the average shear wave velocity to a depth  $H$ . For a layered soil profile:

$$V_{s,avg} = \frac{\sum H_i}{\sum \frac{H_i}{V_{si}}} \quad (3)$$

where  $H_i$  and  $V_{si}$  are the thickness and shear wave velocity of each layer, respectively.

Components of bedrock ground motion having a similar period to the natural site period will be amplified the most at the ground surface.

The customary method for analysing the response of a site to seismic motion at the underlying bedrock is to conduct a one-dimensional (1D) analysis. In such an analysis, only the vertical propagation of seismic shear waves is considered. This is the method used in computer programs such as SHAKE (Schnabel, Lysmer and Bolton Seed, 1972) and DEEPSOIL (Hashash et. al., 2016). Kramer (1996) provides a detailed discussion of the theory and outlines analytical solutions for the special case where the soil damping ratio is assumed constant.

A finite difference time-domain solution, using a program called Earthquake Response of Layered Soils (ERLS), as described by Poulos (1991), calculates the acceleration at different levels in the soil resulting from input earthquake ground motion (acceleration) at the top of bedrock. ERLS discretises the soil profile into a number of connected springs and dashpots, or damped oscillators, as shown in Figure 1 for a very simplified illustrative four element system.

The program solves the equation of motion in the time domain by a forward-marching finite difference process.

ERLS incorporates a strain dependent shear modulus ( $G$ ) and soil damping ( $D$ ). Three parameters are required to account for the strain dependency. These are the small strain damping ratio ( $D_0$ ), the damping ratio at very large strains ( $D_1$ ) and the reference cyclic shear strain ( $\gamma_r$ ).

The strain dependent damping ratio is defined as:

$$D = D_0 + D_1 \left( \frac{\gamma}{1 + \frac{\gamma}{\gamma_r}} \right) \quad (4)$$

and the strain dependent shear modulus as:

$$G = \frac{G_0}{1 + \frac{\gamma}{\gamma_r}} \quad (5)$$

where  $\gamma$  is the cyclic shear strain in the soil.

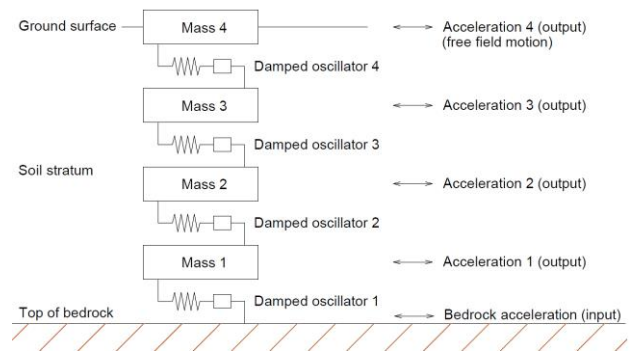


Figure 1. Computational model for 1D site response analysis

In-situ testing for the damping parameters is not common in engineering practice, and published values for typical soils are commonly used. Some recommended values are shown in Table 1. It is strongly advised to check the sensitivity of the results to these parameters.

The bedrock underlying the soil profile contributes apparent damping to the soil, as downward travelling shear waves are partially absorbed by the bedrock. The method of incorporating bedrock damping in ERLS is that outlined by Roesset (1970). The magnitude depends on the natural site period, the predominant frequency of the input earthquake ground motion and the shear wave velocity ratio of the bedrock and soil. Bedrock with a high shear wave velocity results in less damping, and this can have a significant effect on results.

Table 1: Recommended damping parameters

Soil type	$D_0$	$D_1$	$\gamma_r$
Gravelly soils (relative density 80%)	0	0.160	$1.3 \times 10^{-4}$
Quartz sands	0.005	0.260	$3.7 \times 10^{-4}$
Clay (PI 5-10)	0.005	0.265	$4.0 \times 10^{-4}$
Clay (PI 10 - 20)	0.005	0.265	$7.0 \times 10^{-4}$
Clay (PI 20 - 40)	0.005	0.265	$1.1 \times 10^{-3}$
Clay (PI 40 - 80)	0.005	0.265	$2.0 \times 10^{-3}$
Clay (PI > 80)	0.005	0.265	$3.6 \times 10^{-3}$

The authors have re-written ERLS in the Python programming language from its original FORTRAN language.

The computational model for ERLS was not changed during the conversion to Python. However, several new features were added, which include:

- The ability to analyse, apply pile reduction factors and assess the statistics of multiple earthquake input motions in a single run.
- The ability to read common ground motion file formats without pre-processing.
- The creation of reports without post-processing of data.
- The simplification of input parameters.
- A new user interface (currently in development).

Python is a free and open-source programming language with relatively readable syntax and a gentle learning curve.

It is intended that the wide range of open-source statistical, visualisation and even machine learning libraries available with Python will facilitate further research and improvements to the program in the future.

### 3 METHODS OF INCORPORATING PILES INTO THE ANALYSIS

### 3.1 Method 1

Di Laora and de Sanctis (2013) present a method for incorporating the effects of fixed head piles on a two-layered soil profile by applying a reduction factor to the free field response spectra. They introduce a convenient functional form for the spectral ratio between the free field response spectra and the response spectra incorporating piles. The functional form of the spectral ratio is that of two parabolas, as shown in Figure 2. Four constants  $R_0$ ,  $R_{min}$ ,  $T_{min}$  and  $T_{crit}$  are required to construct the curve.

$R_0$  and  $R_{min}$  define the spectral ratio at a period of zero and the minimum spectral ratio.  $T_{min}$  and  $T_{crit}$  are the periods corresponding to the minimum spectral ratio and the period beyond which no significant reduction occurs.

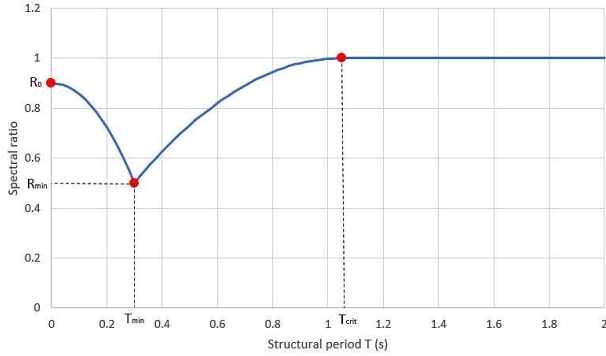


Figure 2. Form of the spectral ratio for fixed head piles

It was shown by Di Laora and de Sanctis (2013) that the ratio of the acceleration at the top and the base of a fixed head pile of diameter ( $d$ ) depends on a dimensionless frequency parameter, which contains information on the pile to soil stiffness ratio, the pile diameter, the frequency of excitation and the shear wave velocity of the soil, defined as:

$$\frac{\omega \lambda_p}{V_s} \quad (6)$$

where  $\omega$  is the circular frequency of the excitation, and

$$\lambda_p = d \left( \frac{E_p}{E_s} \right)^{\frac{1}{4}} \quad (7)$$

The dimensionless frequency, or close variants of it, has been shown to be the key parameter governing pile head response under bedrock seismic loading, which is amplified through a soil profile.

Di Laora and de Sanctis (2013) provide a convenient method for obtaining the constants  $R_0$ ,  $R_{min}$ ,  $T_{min}$  and  $T_{crit}$  shown in Figure 2, as follows:

The average circular frequency of a given input earthquake ground motion is taken as:

$$\omega_s = \frac{2\pi f_m + 2\pi f_p}{2} \quad (8)$$

where  $f_p$  is the frequency with maximum spectral acceleration and  $f_m$  is the mean frequency (Rathje, Abrahamson and Bray, 1998) defined as:

$$\frac{1}{f_m} = \frac{\sum A_i^2}{\sum f_i^2} \quad \text{for } 0.25 \text{ Hz} \leq f_i \leq 20 \text{ Hz} \quad (9)$$

where  $A_i$  is the Fourier amplitude corresponding to  $f_i$ .

The following factor is defined:

$$\Gamma_{t1} = (1 + 0.15 \frac{\omega_s \lambda_p}{V_{s1}})^{-1} \quad (10)$$

where  $V_{s1}$  is the shear wave velocity of the upper layer of a two-layer soil profile with a stiffer lower layer.

It is shown that an upper bound, and hence conservative, estimate is obtained by assuming a homogeneous soil profile with shear wave velocity equal to  $V_{s1}$ . With this assumption, the constants found from a parametric study are:

$$R_0 = 1.71\Gamma_{t1} - 0.64 \quad (11)$$

$$R_{min} = 2.28\Gamma_{t1} - 1.37 \quad (12)$$

$$T_{min} = 12 \frac{d}{V_{s1}} \quad (13)$$

$$T_{crit} = 3.5 T_{min} \quad (14)$$

It is noted that for high circular frequencies ( $\geq 40$  rad/s) and very low shear wave velocities ( $\leq 50$  m/s), the formulae result in negative values for  $R_{min}$  for a typical  $E_p$  of 30 GPa. As such, it is recommended to consider at least 8 input earthquake ground motions and average the results.

### 3.2 Method 2

Turner, Brandenburg and Stewart (2017) provide a comprehensive parametric study building on the work of Di Laora and de Sanctis (2013) and others. They make use of the active length of the pile in the dimensionless frequency parameter. Their results allow for non-homogeneous soil profiles and free head as well as fixed head piles. They adopt the same functional form shown in Figure 2 for a fixed head pile.

Assuming a pile length  $L$ , greater than the pile active length, the procedure for constructing the curve in Figure 2, which is independent of pile diameter, is as follows:

1. Let  $k = \delta E_s$  be the p-y curve initial elastic stiffness, with  $\delta$  being close to 1, say 1.2.
2. Define:

$$\lambda_{La} = \left( \frac{k_{e,La}}{4E_p I_p} \right)^{\frac{1}{4}} \quad (15)$$

where  $k_{e,La}$  is the average value of  $k$  over the pile active length  $L_a$ .

3.  $L_a$  is found iteratively with  $\lambda_{La}$  using the requirement that  $\lambda_{La} * L_a = 4$ . The time averaged shear wave velocity of the soil over the active length  $V_{s,La}$  is then obtained.
4. The predominant frequency  $f_0$  of the input earthquake motion is calculated as the inverse of the predominant period  $T_0$  (Rathje et al., 2004) as follows:

$$T_0 = \frac{\sum T_i \ln \left( \frac{PSA(T_i)}{PGA} \right)}{\sum \ln \left( \frac{PSA(T_i)}{PGA} \right)} \quad (16)$$

for  $T_i$  with  $\frac{PSA(T_i)}{PGA} \geq 1.2$ ,  $\Delta \log(T_i) \leq 0.02$

where  $PSA(T_i)$  are the spectral accelerations at periods  $T_i$  and  $PGA$  is the peak ground acceleration of the input earthquake motion. Note that log denotes the logarithm to base 10 and ln denotes the natural logarithm.

The following three parameters are used to find the constants  $R_0$ ,  $R_{min}$ ,  $T_{min}$  and  $T_{crit}$ :

1. A representation of the dimensionless frequency parameter (6) computed at frequency  $f_0$ :

$$P1 = \frac{f_0}{\lambda_{La} V_{s,La}} \quad (17)$$

2. A parameter quantifying changes in soil stiffness over the pile length:

$$P2 = \frac{V_{s,La}}{V_{s,L}} \quad (18)$$

3. The maximum spectral acceleration of the input earthquake motion normalised by gravity:

$$P3 = \frac{PSA_{max}}{g} \quad (19)$$

For a fixed head pile the four constants,  $R_0$ ,  $R_{min}$ ,  $T_{min}$  and  $T_{crit}$ , are, with log denoting the logarithm to base 10:

$$R_0 = -0.086 \log(P1) + 0.047(P2) - 0.046 \log(P3) + 0.81 \quad (20)$$

$$R_{min} = -0.38 \log(P1) - 0.12(P2) - 0.026 \log(P3) + 0.16 \quad (21)$$

$$T_{min}^{-0.58} = -1.39 \log(P1) + 4.53(P2) + 1.99 \log(P3) - 0.26 \quad (22)$$

$$\log(T_{crit}) = 0.79 \log(P1) - 0.53(P2) - 0.27 \log(P3) + 1.01 \quad (23)$$

and the spectral ratio curve is:

$$R_0 - (R_0 - R_{min}) \left( \frac{T}{T_{min}} \right)^2 : T \leq T_{min} \quad (24)$$

$$1 - (1 - R_{min}) \left( \frac{T_{crit} - T}{T_{crit} - T_{min}} \right)^2 : T_{min} < T \leq T_{crit} \quad (25)$$

$$1 : T > T_{crit} \quad (26)$$

This spectral ratio is applied to a free field motion obtained from a 1D analysis, as outlined in Section 2, to account for the effects of a fixed head pile. Similar equations are available for free head piles, and the reader is referred to the paper by Turner, Brandenburg and Stewart (2017) for details. It is important to note that the effects of a free head pile do not lead to a reduction in response spectra at all frequencies when compared to the free field motion response spectra.

Turner, Brandenburg and Stewart (2017) found that pile group effects were minimal within the parametric bounds of their study. They recommend that a reasonable first order approximation of pile group behaviour could be estimated by reducing the value of the spectral ratio curve by 5%.

#### 4 APPLICATION TO A PROJECT IN SYDNEY

The above process has been applied to a project site in Sydney. The site consisted of a variable thickness of alluvium overlying weathered shale bedrock which can be considered typical of the site conditions found in many parts of Sydney. The overlying structure was a sporting facility on pile foundations, with a natural structural period similar to that of a medium-rise building, around 0.5 s to 1 s. As such, pile foundations were likely to provide beneficial effects in reducing the seismic load on the structure.

Available information on the site consisted of a number of boreholes which provided information on the variability of the depth to bedrock and the thickness of alluvium. This information indicated that the north and eastern parts of the site were classified as Class Ce in accordance with Australian Standard AS1170.4. Based on this, the structural engineers expressed the desire to refine the spectral curves by conducting a site-specific seismic response assessment for the site.

An investigation was carried out consisting of two boreholes drilled to 30 m depth. The boreholes were for the purpose of obtaining shear wave velocity profiles at the two locations. BH01 represented a profile typical the eastern part of the site, and BH02 the northern part. Following drilling, the zone above weathered rock in the boreholes was cased with PVC casing and the annulus filled with a cement-bentonite grout. To obtain reliable shear wave velocity data, it is important there are no air pockets in the annulus. Following completion of the boreholes, a geophone was lowered down the borehole. At half metre intervals, the time was measured at which an impact, made on a railway sleeper positioned on the ground surface near the hole, took to reach the probe. This allowed for an assessment of the shear wave velocity of the material surrounding the borehole. Figure 3 shows the assessed shear wave velocity profile and corresponding shear

modulus profile at the two locations. The shear modulus profile ends at the adopted top of rock level.

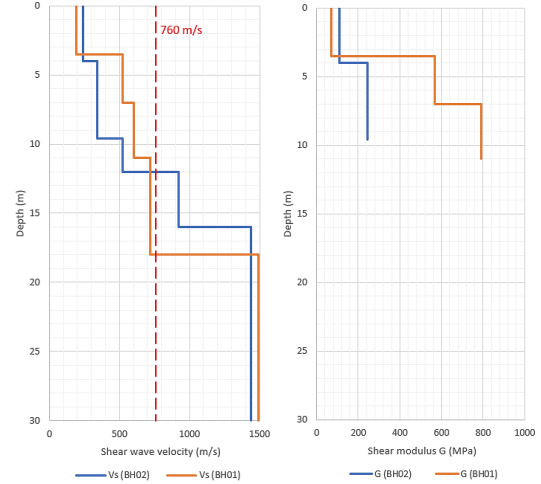


Figure 3: Shear wave velocity and shear modulus profiles at a site in Sydney

Based on the shear wave velocity profile, the natural site period, with  $H$  taken to the adopted top of rock, was found to be 0.13 s at both locations. A deeper adopted top of rock level and lower  $V_s$  in the upper 3.5 m at BH01 resulted in similar natural site periods for both locations. Reduction effects due to piles are usually significant for response spectrum periods less than 0.5 s. This was likely to be beneficial for this site as earthquake ground motion components with periods close to the natural site period of 0.13 s would be amplified the most.

Other parameters were adopted as follows:

- Material unit weights were adopted based on experience.
- Damping parameters  $D_0$ ,  $D_1$  and  $\gamma_r$  were selected based on recommended values, as shown in Table 1.
- The shear wave velocity of the underlying bedrock was adopted as 715 m/s, resulting in a bedrock shear modulus of 1,251 MPa.

The parameters used for the site assessment are shown in Table 2 and Table 3.

Table 2: Parameters adopted for profile at BH01

Layer	Layer thickness (m)	Unit weight (MN/m <sup>3</sup> )	G (MPa)	$D_0$	$D_1$	$\gamma_r$
1	3.5	0.019	69	0.005	0.26	$3.7 \times 10^{-4}$
2	3.5	0.021	568	0.0005	0.265	$1.1 \times 10^{-3}$
3	4.0	0.022	792	0	0.16	$1.3 \times 10^{-4}$
Bedrock	Not proven	0.024	1250	n/a	n/a	n/a

Table 3: Parameters adopted for profile at BH02

Layer	Layer thickness (m)	Unit weight (MN/m <sup>3</sup> )	G (MPa)	$D_0$	$D_1$	$\gamma_r$
1	4	0.019	110	0.005	0.26	$3.7 \times 10^{-4}$
2	3.8	0.021	245	0.0005	0.265	$1.1 \times 10^{-3}$
3	1.8	0.022	245	0	0.16	$1.3 \times 10^{-4}$
Bedrock	Not proven	0.024	1250	n/a	n/a	n/a

A dataset of 115 ground motion records was downloaded from the Pacific Earthquake Engineering Research Center (PEER) database, satisfying the following two criteria:

- Magnitude = 6.5
- Epicentral distance = 30 km.

These criteria were selected to obtain a consistent set of input ground motion records. Hoult, Lumantarna and Goldsworthy (2013) reported that the above magnitude-distance relationship is consistent with a 1 in 2500 year return period earthquake for



Sydney, although the authors noted that this does have very little statistical basis.

From this set, a smaller set of 34 ground motion records was randomly selected from those having peak ground acceleration between 0.05g and 0.15g. These 34 ground motions were then scaled to a peak ground acceleration equal to 0.08g.

An assessment of seismic amplification was carried out using ERLS with a pile reduction factor applied based on the method of Turner, Brandenburg and Stewart (2017) described above in Section 3.2. The results for the 34 individual ground motion records were then averaged and compared to the site classification classes Be and Ce as described in AS1170.4. The results are shown in Figure 4 and Figure 5. Figure 6 shows the pile reduction factor for selected periods for the profile at BH01.

Based on these results, the structural engineers were recommended to adopt a site subsoil class Be for the eastern part of the site, covered by the profile at BH01, instead of the more onerous site subsoil class Ce, which would have been required if no seismic site assessment was carried out. It can be seen from the figures that in both locations the seismic demand on the structure is reduced noticeably for periods below 0.3 if the effects of piles are incorporated into the assessment. These periods are most relevant to low rise buildings.

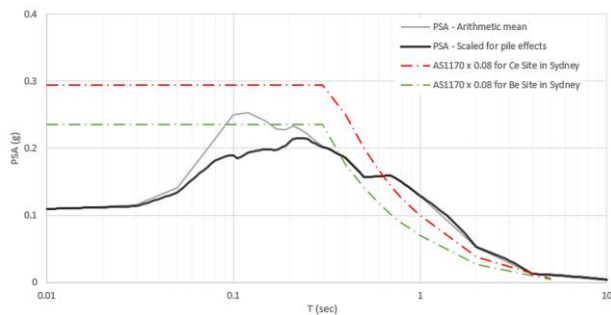


Figure 4: Seismic response spectrum (profile at BH01)

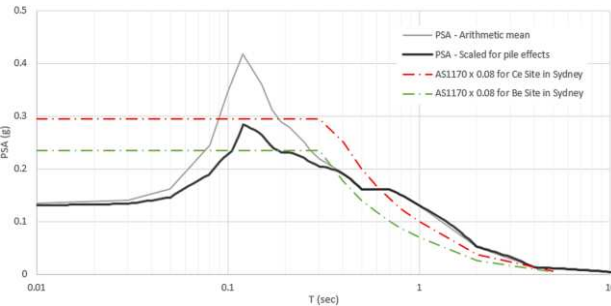


Figure 5: Seismic response spectrum (profile at BH02)

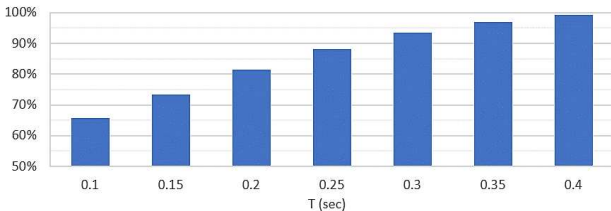


Figure 6: Pile reduction factor for selected periods (profile at BH01)

## 5 CONCLUSIONS

In engineering practice, it is common to ignore the effects of pile foundations when conducting a seismic site assessment. This can lead to conservative results, particularly for response spectrum periods below 0.5 s. This is especially the case where the natural site period is less than 0.5 s.

A procedure has been outlined whereby a reduction factor may be applied to the free field response spectrum to incorporate the effects of piles. The reduction factor is governed by a dimensionless frequency parameter which incorporates the pile to soil stiffness ratio, the shear wave velocity of the soil and the mean frequency of the earthquake ground motion.

The application of the method to a project site in Sydney was discussed. The results show that the incorporation of the effects of piles led to a substantial reduction in the seismic demand on the structure compared to both the design code and the free field seismic response spectrum.

## 6 REFERENCES

- Di Laora, R., and de Sanctis, L. 2013. Piles-induced filtering effect on the Foundation Input Motion, *Soil Dynamics and Earthquake Engineering* 46(2013) 52-63.
- Hashash, Y., Park, D., and Tsai, C. C., Philips, C., and Groholski, D.R. 2016, "DEEPSOIL - 1-D Wave Propagation Analysis Program for Geotechnical Site Response Analysis of Deep Soil Deposits, Version 6.1", Tutorial and User Manual, University of Illinois at UrbanaChampaign.
- Hoult, R., Lumantarna, E., and Goldsworthy, H.M. 2013. Ground Motion Modelling and Response Spectra for Australian Earthquakes. Proc. 2013 Australian Earthquake Engineering Society Conference, Australian Earthquake Engineering Society.
- Kramer, S.L. 1996. *Geotechnical Earthquake Engineering*. Prentice Hall.
- Poulos, H.G. 1991. *ERLS User's Manual*. Coffey Partners International, Sydney.
- Rathje, E.M., Abrahamson, N.A., and Bray, J.D. 1998. Simplified frequency content estimates of earthquake ground motions, *J. Geotech. Geoenviron. Eng.*, 1998, 124(2), 150-159
- Rathje, E.M., Faraj, F., Russell, S., and Bray, J. D. 2004. Empirical Relationships for Frequency Content Parameters of Earthquake Ground Motions, *Earthquake Spectra* Vol. 20, No. 1, 119-144.
- Roesset, J.M. 1970. Fundamentals of soil amplification, *Seismic Design for Nuclear Power Plants*. Hansen, Robert J. (ed.) 183-244, Massachusetts Institute of Technology Press.
- Schnabel, P.B., Lysmer, J., and Bolton Seed, H. 1972. SHAKE, a computer program for earthquake response of horizontally layered sites, *Earthquake Engineering Research Centre, Report No. EERC 72-12*
- Turner, B.J., Brandenburg, S.J., and Stewart J.P. 2017. Influence of Kinematic SSI on Foundation Input Motions for Bridges on Deep Foundations, *PEER Report No. 2017/18*.

## 7 APPENDIX

The appendix provides a comparison of results from ERLS and DEEPSOIL. Note that a pile reduction factor was not applied to the ERLS results.

### A.1 Soil profiles

Four hypothetical profiles, each consisting of 15 m of uniform soil overlying bedrock ( $V_{s(rock)} = 760$  m/s) were used for the comparison. The soil for each of the profiles was assigned a different shear wave velocity ( $V_s$ ). The damping parameters were the same for all profiles, along with the unit weight of the soil (20 kN/m<sup>3</sup>). Table 4 shows the input parameters for ERLS.

Table 4: ERLS input parameters and natural site periods for the four profiles

Soil	$V_s$ (m/s)	$D_0$	$D_1$	$\gamma_r$	Natural site period
Profile 1	75	0.005	0.265	$1.1 \times 10^{-3}$	0.80
Profile 2	150	0.005	0.265	$1.1 \times 10^{-3}$	0.40
Profile 3	250	0.005	0.265	$1.1 \times 10^{-3}$	0.24
Profile 4	500	0.005	0.265	$1.1 \times 10^{-3}$	0.12

Using (4) and (5), curves representing the strain dependent damping ratio and strain dependent shear modulus were used to represent the profiles in DEEPSOIL (time domain non-linear, MKZ with Masing rules). This was achieved by providing discrete input points and simultaneously fitting both the modulus and damping curves using the curve fitting function in DEEPSOIL. The fit was reasonable, although not exact.

Each profile was discretised into 15 elements of 1 m thickness in both ERLS and DEEPSOIL.

## A.2 Input ground motion records

A set of 303 earthquake ground motion records were downloaded from the Pacific Earthquake Engineering Research Center (PEER) database, satisfying the following two criteria:

- Magnitude between 5.5 and 7.5
- Epicentral distance between 20 km and 60 km

A set of eight horizontal ground motion records were randomly selected from the larger set, with the criteria that each related to a different earthquake event and that each had a peak ground acceleration of between 0.6g and 0.15g. Table 4 provides details of the selected ground motion records.

Table 4: Input ground motion records

Event	$T_{char}^{(1)}$	PGA <sup>(2)</sup> / g	Filename
Little Skull MtnNV	0.30	0.09	RSN1741_SKULLMTN_LSM2270.AT2
Hector Mine	0.32	0.08	RSN1795_HECTOR_JTN090.AT2
Irpinia Italy-02	0.34	0.1	RSN302_ITALY_B-VLT270.AT2
Morgan Hill	0.38	0.07	RSN471_MORGAN_SJL360.AT2
N. Palm Springs	0.12	0.07	RSN541_PALMSPR_H02000.AT2
Taiwan SMART1(45)	0.43	0.14	RSN572_SMART1.45_45EO2EW.AT2
Whittier Narrows-01	0.29	0.13	RSN596_WHITTIER.A_A-MU2122.AT2
Landers	0.19	0.06	RSN897_LANDERS_29P090.AT2

1.  $[0.5 * (f_m + f_p)]^{-1}$ , refer to Section 3.1
2. Peak ground acceleration

## A.3 Results

Figure 7 to Figure 10 show the assessed median surface response spectra of the eight input ground motion records. A structural damping of 5% was used in the assessment.

The figures also include results for an analytic solution with constant soil damping of 5%. This solution is provided by Kramer (1996), equation 7.11.

The results from ERLS and DEEPSOIL can be seen to be reasonably consistent.

At Profile 1 and Profile 2, for spectral periods greater than approximately 0.2 s, the ERLS results are conservative in comparison to DEEPSOIL, with the discrepancy appearing to be larger for sites with a higher natural site period. At these sites, non-linearity is more apparent. The representation of soil damping is slightly more simplified in ERLS than DEEPSOIL, and this is likely the reason for the difference in results.

For spectral periods below approximately 0.15 s, the ERLS results are non-conservative in comparison to DEEPSOIL. The reason for this is not clear.

For pragmatic approaches to design in engineering practice, the authors consider ERLS, with its conceptually simple representation of soil damping and related program inputs, to be suitable. It is recommended to exercise caution for results at spectral periods less than 0.15 s and similarly for locations with a natural site period greater than 0.6 s.

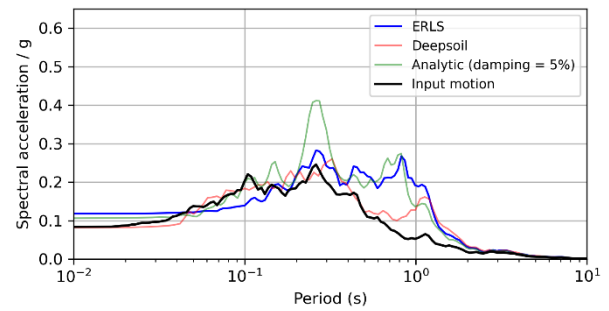


Figure 7: Comparison of median surface response spectra, Profile 1

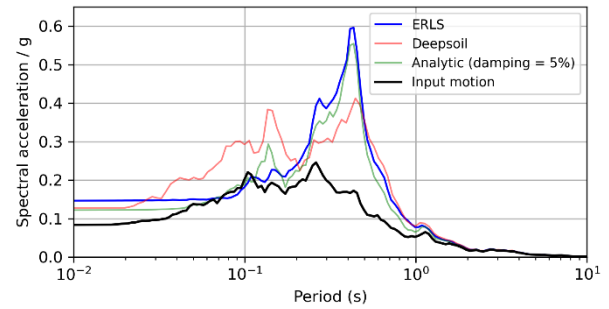


Figure 8: Comparison of median surface response spectra, Profile 2

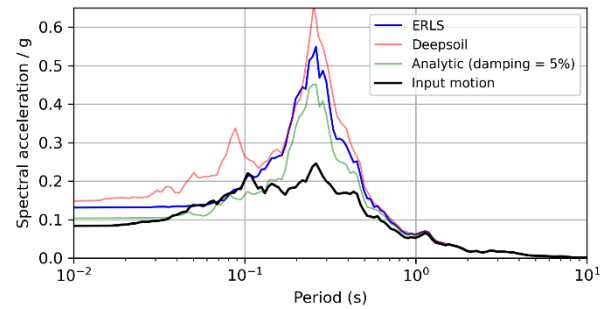


Figure 9: Comparison of median surface response spectra, Profile 3

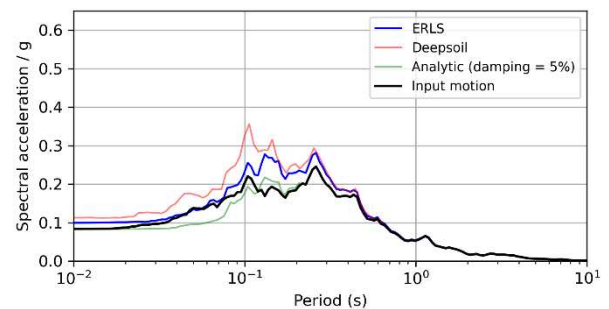


Figure 10: Comparison of median surface response spectra, Profile 4